Finite Element Modelling of Orthopaedic Implants using Metal Foam

G. L. Manco[a], K. Datta[b], J. William[c], T. Momen[d], D. Umbrello[a], F. Gagliardi[a]

[a]Department of Mechanical Engineering, University of Calabria, 87036 Rende (CS), Italy

[b]Data Metallurgical Company, Consulting Engineers, 28 Townshend Road, Kolkata 700 025, India

[c]Dassault Systemes Simulia B.V. - Safariweg 14-16, 3605 MA, Maarssen- The Netherlands

[d]Consultant Orthopaedic Surgeon, 30 Circus Avenue, Kolkata 700017, India

Abstract: Cellular structures like metal foam have several interesting attributes to mimic the properties of human bone for designing orthopaedic implants. A finite element method (FEM) analysis of the forging process of a simple-shaped metallic foam billet is carried out using mathematical models in order to obtain a 3D geometry of a complex form. In particular, the deforming behaviour of a metallic foam and the development of density gradients are investigated in order to produce a selected portion of a hip prosthesis, for replacement of human bone. Abaqus v6.8 code is used and the results are compared with previously done experiments. The complex 3D structure is successfully modelled. The constitutive model of the porous material is used. The model is validated by the comparison of the predicted results with the experimental evidence. Forged metallic foam stands out in its ability to control the size and distribution of the pores during forging to manipulate the strength of the finished implant. When appropriately coated, it also offers better fixation in cementless joint replacement by triggering bone ingrowth.

Keywords: Biomedics, FEM, Metal Foam, Prostheses

1. Introduction

The real motivation behind this study was to investigate a relatively new class of functional material namely cellular metals as a prospective material for bioimplants. Finite Element Method (FEM) analysis provides a good numerical modelling method to investigate manufacturing methods and protocols in detail at the design stage. FEM has reached a mature and advanced stage where several good softwares are available for engineering analyses. The mechanics of elasto-plastic flow in cellular solids being very specific and somewhat different from the flow in pure solids, it was envisaged to compare various available FEM codes to simulate cellular metal forming. This is a sequel to previous studies using the commercial codes Deform3D and LsDyna. In this article, the model is built with the commercial code Abaqus v6.9.

2. Constitutive behavior of metal foams

In order to define the deformation behavior of metallic foam, a phenomenological constitutive law was developed by Deshpande and Fleck [1]. Onck [2] studied the behavior of double-edge notched specimens of metallic foams in compression, numerically, using this constitutive law. Compressive yielding in response to hydrostatic stress is incorporated through a dependence on the plastic Poisson ratio ν^p. A summary of the model is given below.

Employing the fact that foams yield in response to both hydrostatic loading as well as deviatoric loading, a yield surface is defined by

$$\phi = \hat{\sigma} - Y \qquad (1)$$

where Y is the yield stress and $\hat{\sigma}$ is an equivalent stress measure defined as

$$\hat{\sigma}^2 = \frac{1}{\left[1+\left(\alpha/_3\right)^2\right]}\left(\sigma_e^2 + \alpha^2\sigma_m^2\right) \qquad (2)$$

with $\sigma_e = (\frac{3}{2}\sigma'_{ij}\sigma'_{ij})^{1/2}$ the von Mises effective stress, σ'_{ij}, the Cartesian components of the stress deviator and $\sigma_m = \frac{1}{3}\sigma_{kk}$, the mean stress. Clearly, (1) defines an ellipse in (σ_m, σ_e) space, with its shape determined by the phenomenological parameter α. One of the attractive features of this yield surface is that the parameter can be linked to the plastic Poisson ratio ν^p in a uniaxial compression test:

$$\nu^p = -\frac{\dot{\epsilon}_{11}^p}{\dot{\epsilon}_{22}^p} = \frac{\left(\frac{1}{2}\right)-\left(\frac{\alpha}{3}\right)^2}{1+\left(\frac{\alpha}{3}\right)^2} \qquad (3)$$

Where $\dot{\epsilon}_{11}^p$ and $\dot{\epsilon}_{22}^p$ are the plastic strain rate perpendicular and parallel to the direction of compression, respectively. For $\alpha = \sqrt{4.5}$, we have $\nu^p = 0$, meaning that no lateral expansion will occur upon compressing the specimen uniaxially. For
α=0 we have ν^p=0.5, corresponding to incompressible plasticity, $\hat{\sigma}$ reduces to σ_e and J_2 flow theory is recovered. Note that the plastic Poisson ratio increases with relative density, such that ν^p=0.5 no longer corresponds to a metallic foam, but to the limit of a dense metal. Typical values for the plastic Poisson ratio for low-density foams are in the range between 0 and 2.5. Gioux et al. [3] report ν^p=0.052 for an open-cell foam (Duocel, 7% relative density) and ν^p=0.024 for a closed-cell foam (Alporas, 8%). Deshpande and Fleck [1] report slightly different values: ν^p=0.013(Alporas, 8.4%), ν^p=0.174 (Duocel, 7%) and ν^p=0.247 (Alporas, 13%). Assuming associated flow and

$$\dot{\epsilon}_{ij}^p = \frac{\dot{Y}}{H}\frac{\partial\phi}{\partial\sigma_{ij}} \qquad (4)$$

with H , the hardening modulus related to, $\dot{\hat{\epsilon}}$ the plastic work rate-conjugate to $\hat{\sigma}$, by

$$H = \frac{\dot{\hat{\sigma}}}{\dot{\hat{\epsilon}}} \qquad (5)$$

The equivalent strain rate $\dot{\hat{\epsilon}}$ can be expressed in terms of the effective plastic strain rate

$$\dot{\epsilon}_e = (\frac{2}{3}\dot{\epsilon}_{ij}^{\prime p}\dot{\epsilon}_{ij}^{\prime p})^{\frac{1}{2}} \qquad \text{and}$$

the volumetric plastic strain rate

$$\dot{\epsilon}_m = \dot{\epsilon}_{kk}^{p} \qquad \text{as}$$

$$\dot{\hat{\epsilon}}^2 = \left[1 + \left(\frac{\alpha}{3}\right)^2\right]\left(\dot{\epsilon}_e^2 + \frac{1}{\alpha^2}\dot{\epsilon}_m^2\right) \qquad (6)$$

It is assumed that hardening is isotropic so that the yield surface as given by Eqs. (1) and (2) evolves in a self-similar manner. The hardening modulus H is obtained from a uniaxial compression test for which $\hat{\sigma}$ reduces to the applied Cauchy stress σ and $\hat{\epsilon}$ to the uniaxial compressive logarithmic plastic strain ε. Then, H is the slope of the Cauchy stress-logarithmic strain curve at strain level ε :

$$H(\epsilon) = \frac{\dot{\sigma}}{\dot{\epsilon}} \qquad (7)$$

The hardening response can be obtained from a uniaxial compression test which can be input to a FEM code.

In another attempt, a thermodynamically consistent approach is developed by Hård af Segerstad et al. [4] for modelling the response of an open-cell cellular solid at finite compressive strains. The model is well capable of reproducing data from compression experiments on various open-cell aluminium foams.

Mulalo Doyoyo and Tomasz Wierzbicki [5] reveal that the specimen size effects are a major cause of the unreliability of foam models in finite element codes. They found that as the foam's internal structure is inhomogeneous, and so is the deformation field, strain localization and failure can occur at any weak layer of cells in the bulk. Phenomenological yield surfaces, which incorporate these features are obtained for the foams, and show dependence on both the deviatoric and hydrostatic stresses. They also provide expressions for the shear and hydrostatic strengths in terms of the uniaxial strengths. Finally, the size-independence of the yield surface is verified using the uniaxial compression of tapered specimens.

Peroni et al. [6] found that among the various aspects still to be investigated regarding mechanical behavior of the foam was the influence of a hydrostatic state of stress on yield strength. Unlike metals, the hydrostatic component affects yields. Therefore, different loading conditions have to be considered to fully identify the material behaviour. Another important issue in foam structure design is the analysis of composite structures, e.g. metal foam sandwiched between two solid metal plates. The results show that the energy absorption capability of the composite structures is much greater than the sum of the energy absorbed by the two components, i.e. the foam and the plate.

Schmidt [7] modeled and simulated the deformation induced elasto-plastic anisotropy in metal foams. The internal variable framework for the description of elasto-plastic material behaviour in the presence of anisotropy is briefly reviewed. Some existing formulations of anisotropic plasticity are compared, discussing in particular the formulations of the normality rule and the assumptions regarding the elastic behaviour. The author presented the simulated response, obtained by numerical homogenisation of a two dimensional cellular model material to selected straining paths. It is found that the elastic and plastic anisotropies are closely related and do not differ significantly from an orthotropic symmetry whose axes coincide with the principal plastic stretch directions, even for strongly non-proportional loading paths.

Badiche et al. [8] applied the mechanics of cellular solids and porous materials to non-homogeneous deformation of open cell nickel foam. The obtained Young's modulus, compression yield stress and tensile fracture stress are compared to the predictions of models based on periodic, Penrose and Voronoi beam networks. It was found that Gibson and Ashby's model [9] provided the proper scaling laws with respect to relative density for almost all investigated properties. The strong anisotropy of the observed overall responses could also be accounted for. The two-dimensional strain field during the tension of a nickel foam strip had been measured using a photomechanical technique. Non-homogeneous deformation patterns were shown to arise. The same technique was used to obtain the strain field around a circular hole in a nickel foam strip. The observed deformation fields were compared to the results of a finite element analysis using anisotropic compressible continuum plasticity.

Chen and Lu [10] worked on a phenomenological framework of constitutive modelling for incompressible (grey cast iron) and compressible (metal foams) elasto-plastic solids. The different yielding behaviours under tension and compression as well as differential hardening along different loading paths were accounted for in a relatively simple manner. The predicted yielding behaviours for grey cast iron and metal foams compare favourably with those measured.

Chen and Fleck [11] studied the size effects in the constrained deformation of metallic foams. The deformation response of the aluminium foam layer was modelled by the elastic–plastic finite element analysis of regular and irregular two dimensional honeycombs, bonded to rigid face sheets; in the simulations, the rotation of the boundary nodes of the cell-wall beam elements was set to zero to simulate full constraint from the rigid face sheets. It is found that the regular honeycomb under-estimates the size effect whereas the irregular honeycomb provides a faithful representation of both the observed size effect and the observed strain profile through the foam layer. Additionally, a compressible version of the Fleck–Hutchinson strain gradient theory was used to predict the size effect; by identifying the cell edge length as the relevant microstructural length scale, the strain gradient model is able to reproduce the observed strain profiles across the layer and the thickness dependence of strength.

J. Hohe and W. Becker [12] studied the Geometrically nonlinear stress–strain behaviour of hyperelastic solid foams. The model is applied to an analysis of the effective stress–strain behavior of two-dimensional model foams with periodic and disordered microstructure. Special interest is directed to effects of the geometric nonlinearity.

3. The porous material model used in Abaqus

In ABAQUS [13], the porous metal plasticity model is used to model materials with a dilute concentration of voids in which the relative density is greater than 0.9. It is based on Gurson's porous metal plasticity theory by Gurson [14] with void nucleation and, in Abaqus/Explicit, there is a failure definition; and the model defines the inelastic flow of the porous metal on the basis of a potential function that characterizes the porosity in terms of a single state variable, the relative density. For a metal containing a dilute concentration of voids, Gurson [15] proposed a yield condition as a function of the void volume fraction. This yield condition was later modified by Tvergaard [14] to a modified form. In Abaqus/Standard, the implicit code, the accuracy of the implicit integration of the void nucleation and growth equation is controlled by prescribing the maximum allowable time increment in the automatic time incrementation scheme.

4. FEM Modelling

Finite Element Method (FEM) is a versatile numerical modeling technique for engineering design. It enables in carrying out stress-strain analyses. When a material is formed to create a desired product, it goes through an evolution of stress-strain fields in it that also affects its internal microstructure and therefore, the mechanical and physical properties. An integrated engineering design takes care of these variables and FEM helps in visualizing these changes and helps in controlling the parameters for optimal design. FEM has been successfully used to model biomedical prostheses as well as to study various soft-tissue related mechanics while the prosthesis is inside the body. In this section, a few recent applications of FEM in designing biomedical implants are discussed.

A new dimension to inducing specific properties of bone in an implant is revealed when Gagliardi et al. [16, 17] and Filice et al. [18] tried to forge metallic foam to tailor make specific parts of hip prosthesis. The deforming behaviour of a metallic foam and the development of density gradients were investigated through a series of experimental forging tests in order to produce a selected portion of a hip prosthesis. This type of replacement for human bone was chosen as object of study due to its elevated commercial demand and its particularly complex 3D shape. They used FEM to model the forging process and compared with experimental observations. Different available numerical codes were used : Deform 3D, LS-Dyna etc. The usefulness of the model used was verified by the comparison of the predicted results (the force necessary for the completion of the forging process and the final shape obtained) and the experimental evidence. Metallic foams are new materials mainly produced by expansion in a proper chamber and mainly characterized by internal voids: a material characterized by a very low density is obtained in this way. A lot of foamed components are commonly produced, directly by injecting a gas or foaming agent into molten metal inside a closed die. However, secondary operations on these materials can play an important role in order to enhance the foam production flexibility. From the above considerations, the deformation behaviour of an aluminium foam was investigated by compression tests. The study basically compares three different FE strategies and formulations for numerical analyses highlighting their points of strength and weakness in order to verify their applicability in process design. In this paper, the study carried out with Abaqus code is presented.

5. Surgical Procedures

The commonest surgical procedures performed in orthopaedics surgery are hip, knee arthroplasties and osteosynthesis of bones involving implants. Hip arthroplasty is the gold standard, introduced by Sir John Charnley. It is indicated for replacing damaged or broken joint with prosthetic joints which will function like a normal ball and socket hip joint. The commercial hip prosthesis has three parts

i) Acetabular socket
ii) Head
iii) Stem.

Each individual part needs to be appropriately sized. The materials used are diverse, ranging from titanium, to ceramic, to stainless steel. The method of fabrication used is either cemented or uncemented. For cemented hip replacement, the acetabular and stem are coated with antibiotic coated cement for rigid fixation. Uncemented prostheses are coated with Hydroxyapatite which encourages bone growth and are press-fit. The main complications of hip replacement are

a) Loosening of prosthesis
b) Wear of prosthesis
c) Metallic reaction in the body.

Knee replacement for the last thirty to forty years has revolutionized the treatment of osteo-arthritis of the knee. It is more of a re-surfacing of the damaged articular surface of femur + tibia + patella, than full replacement. The prostheses are either made of titanium, cobalt-chrome, stainless steel and high molecular weight plastic. Standard anterior, para-patellar incisions are used. Again the prosthesis may be either cemented or non-cemented.

Common complications seen are

a) Loosening
b) Mal-position
c) Infection
d) Wear and tear of the prosthesis.

A novel implant material like titanium foam may help in improving the quality and reducing complications.

6. Industrial case study

6.1 Introduction

In general, the interest in metallic foams has grown quickly bringing to excellent results in innovative parts where, for example, low weight, high stiffness and high energy absorption are strict design parameters [19,20]. However, there is a considerable lack of knowledge in the characterization of the macroscopic behaviour of foams, especially when 3D complex shapes are considered. For this reason, the aim of the present study is to investigate the effectiveness of mathematical modelling when compared to experimental evidence; to do this, a portion of a commercial hip prosthesis was considered to carry out both the estimation of the registered punch load and the final shape of the forged component. An innovative approach is being developed by the Faculty and research engineers at the Department of Mechanical Engineering of the University of Calabria [16-18] using foams as materials instead of solids to manufacture biomechanical parts that have the same density and stiffness of natural bones.

6.2 Material

The optimal materials to be used are obviously titanium alloys or stainless steel. Unfortunately, foams obtained from such materials have been unavailable up to now on the worldwide market, although there are several studies oriented towards the production of titanium foams [21]. This study was carried out using aluminium foam even if, this alloy is not bio-compatible and will never be used to produce bone replacements. However, the flowage mechanism allows for the acquisition of a more general methodology that, in the future, could be extended to other materials more suitable for implant manufacturing for humans.

For the present study, an Alulight® foam [22] was selected. It is an Al6061-O foam containing 1% magnesium and 0.6% silicon (UNI AlMg1Si0.6); this material is available in cylinders with a relative density ranging from 0.1 to 0.4. Pores have several shapes with different sizes, which are generally closed, having an equivalent diameter from 0.5 to 5mm(Fig.1).

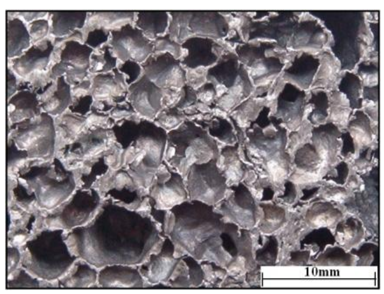

Figure 1 Structure of the worked aluminium foam [16].

6.3 Investigated problem

The hip implant is characterized by highly varied mass distribution along its axis, as can be seen in Fig. 2. The portion of the prosthesis investigated was selected according to the research on fatigue failure of hip–bone implant developed by Raimondi and Pietrabissa [23]. More in detail, the hip portion was chosen around the so-called “critical section” which is the area subjected to the highest Von Mises stress and located directly below the main bending portion (Fig. 3).

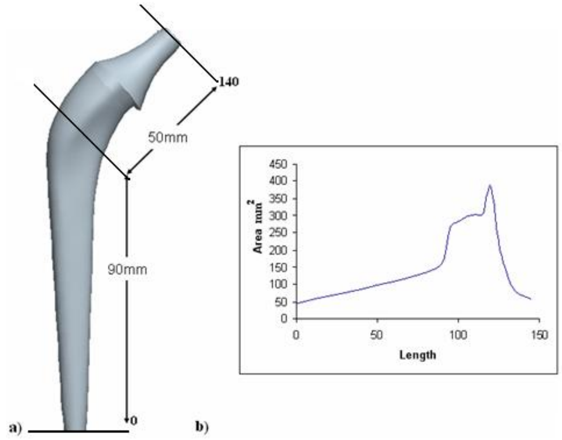

Figure 2 (a) Commercial hip; (b) material distribution along the hip axis [16].

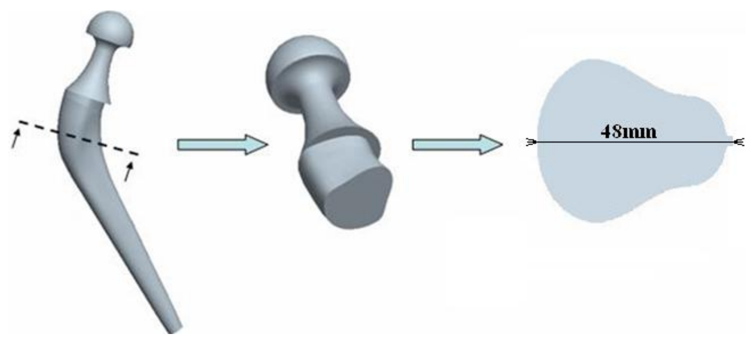

Figure 3 Location of critical area and cross-section [16].

7. Finite Element Modelling

This problem has been thoroughly investigated using two commercial codes Deform3D® [16] and LS-Dyna ® [17]. In this particular study, the same problem is investigated with the help of another commercial FE code Abaqus v6.9. This is pre-cursor to an extensive benchmarking study that the authors are embarking upon.

7.1 Constitutive Equation

The flow stress in MPa at room temperatures can calculated from the following constitutive equation, derived from tensile tests on specimens cut from Al6061-O solid material.

$$\sigma = 210\varepsilon^{0.2} \qquad (20)$$

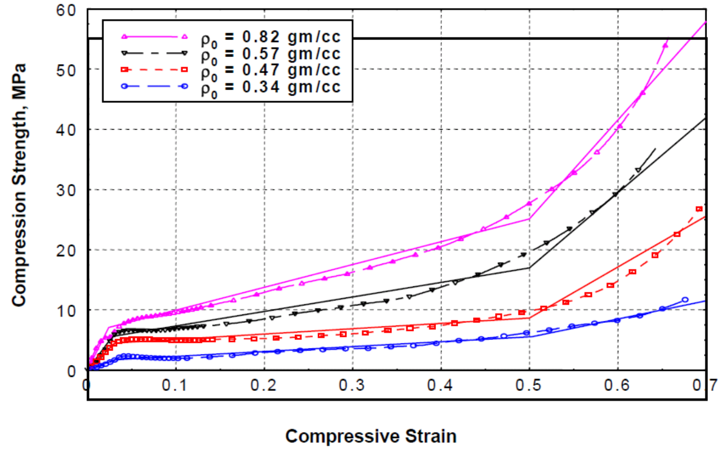

Figure 4 Quasi-static compressive behavior of 6061 Al foam [22].

The quasi-static compressive strength of 6061 Al foam is obtained from the manufacturer [22] of the foam . Fig. 4 shows the variation in compressive strength of this foam with porosity. The compressive strength of any metal foam can be tailored by varying the foam density. The properties of the foam can also be modified by the selection of the alloy composition and heat treatments. The stress-strain data were obtained from these curves and were used in the material modelling.

The POROUS option in Abaqus material module can be used to model metallic foam, or the relative density of the foam can be used and updated with every integration during deformation. The die and the punch material are assumed to be rigid bodies defined by rigid surfaces. Furthermore, great attention was paid in defining the local density distribution in the meshed billet by the application of the image processing analysis (IPA) technique, proposed by some of the present authors [18]. According to the IPA technique, it was possible to introduce in the FE analysis the average density distribution as a function of the billet radius. This assumption was possible because the density distribution does not vary substantially in different sections. Furthermore, owing to the IPA technique and by regression analysis, the following full density law was calculated:

$$\rho = 0.234\, r^3 - 7.180\, r^2 + 73.343\, r + 80.646 \text{ (kg/m}^3\text{)} \qquad (21)$$

where r is the investigated foam radius (without deformations). This formula was used to define an initial density distribution across the billet cross section.

7.2 Contact

The friction modelling is carried out with a simple model based on the constant shear hypothesis: f_s = mk was implemented . In the above model f_s is the frictional stress, k the shear yield stress and m is the frictional factor. The latter was set equal to 0.75 according to Manisekar et al. [24], who investigated a cold compression process without any lubrication. In order to find out the effect of changing die-metal friction on the stress-strain profile of the deforming foam billet, the frictional factor was varied so as to obtain a range of surface condition from slipping to sticking conditions.

7.3 Boundary Conditions

The punch is moved down at a fixed speed. The die is held static with encastering both translation and rotation. The general static analysis is performed using Abaqus Standard's explicit formulations.

8. Results and discussion

A 25 mm radius aluminium foam is modeled in 3D using a 28 mm billet thickness. The geometry of the hip replacement section is curved out in the die and the punch (Fig. 5, middle). Finally, the die and the punch are defined as rigid body surfaces. The analysis is carried out with a general dynamic procedure with the punch closing at a specific velocity. The explicit solver is applied. An accurate input of the constitutive equation for the foam is the key to getting realistic outputs from the model. With a non-linear geometry, the contact also plays a key role in converging the solutions. A realistic estimate of the die-metal and punch-metal contact is essential for this purpose.

An Aluligh® foam was selected. It is an Al6061-O foam containing 1% magnesium and 0.6% silicon (UNI AlMg1Si0.6) [22]; Experiments were carried out in the laboratory using this material. It is available in cylinders with a relative density ranging from 0.1 to 0.4. Pores have several shapes with different sizes, which are generally closed, having an equivalent diameter from 0.5 to 5mm (Fig. 1). Fig. 2 shows the billet, the die and the assembly during the experiment. The equivalent FEM model geometry is shown in Fig. 6.

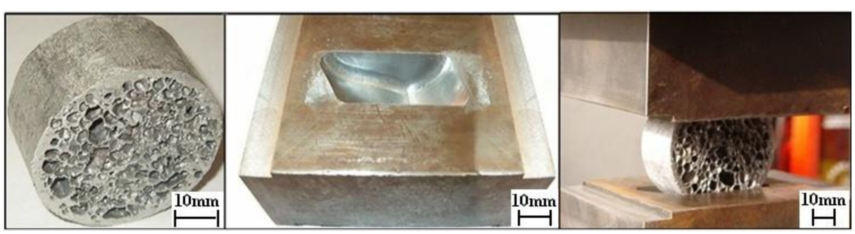

Figure 5 Initial foam billet (left), bottom die (middle) and initial forging sequence (right) [16].

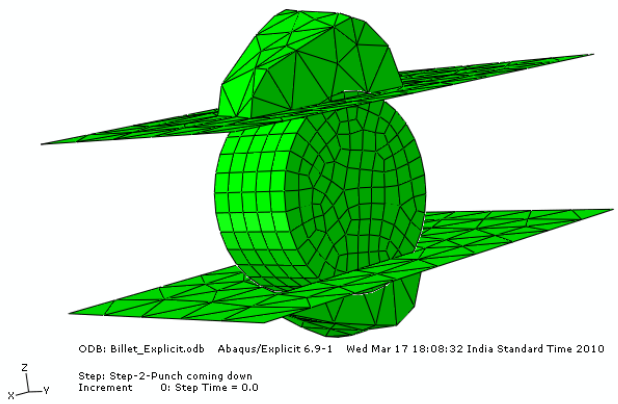

Figure 6 The geometry of the model of die-punch and billet.

The first set of analyses is carried out using the exact experimental conditions in the numerical model so as to validate the results from the model. The two basic validation parameters were the deforming shape of the billet at various stages during forging and, more precisely, the force-displacement pattern during forging. The final shape and size of the flash (the excess material flowing out at the centre) are also compared with that obtained from the model for the purpose of validation. Fig. 7 shows the actual billet sections at different stages during forging vis-à-vis the corresponding cross sections obtained from the model. Fig. 8 compares the flash between the experiment and the model. It is thus observed that both the evolving contour as well as the final shape of the flash as obtained from the FEM model is in agreement with the experiments. However, a more quantitative parameter to compare is the force-displacement behavior, as the punch closes on to the die. Fig. 9 depicts the comparison of force-displacement curves between experiment and models. While the order of magnitude of the force matches, there are portions where force is under predicted and there are portions, towards the later stages, when force is over predicted by the model. The reason for this could lie mostly in the definition of stress-strain data in the numerical model. The data used were generated by using quasi-static compressive tests and they were not done on the same cast of the Alulight foam. So the discrepancy in actual and predicted force-displacement curve could owe to the flow stress data used for the foam.

(a)

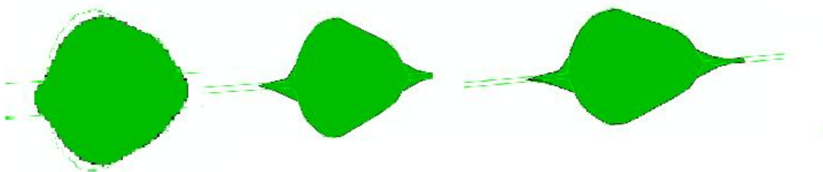

(b)

Fig. 7 (a) Deformed billet at 50% (left), 75% (middle) and 100% (right) of the assigned die stroke [16]. (b) Corresponding sections from the model.

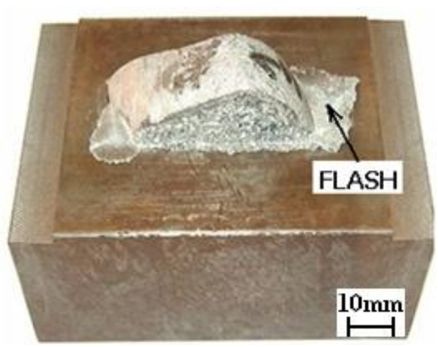

(a)

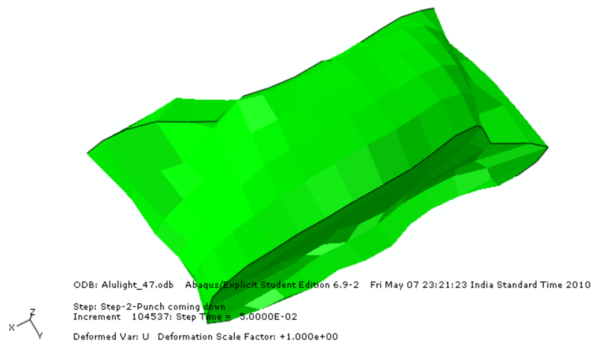

(b)

Figure 8 (a) The foam billet at the end of forming process [16]. (b) The flash as seen from the model after forging.

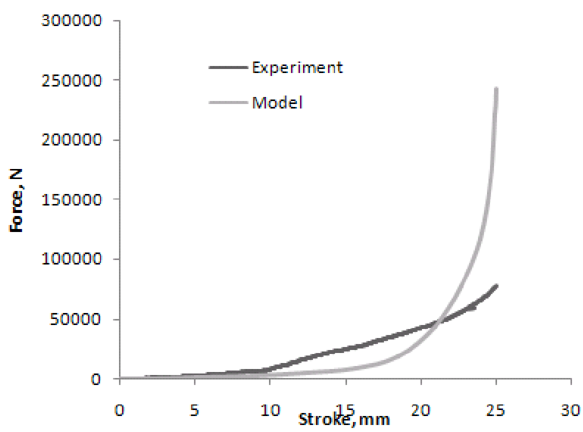

Fig. 9 Comparison of force-displacement behavior between experiment and model.

9. Conclusion

The quality of implants is fundamental to improve the quality of life for many people. For this reason, manufacturing biologically compatible hip prostheses has gained growing attention in the recent years. The real innovation consists of the raw material used, which according to the proposed approach is a metallic foam instead of solid billets. In fact, the use of this type of material can reduce the stiffness of the prosthesis, which is usually higher in currently available prostheses compared to that of human bone, and often leads to implant loosening. According to the results obtained, it is possible to state that the commercially available implicit FE codes, based on the updated Lagrangian formulation, can be applied to reproduce the forging process with notable accuracy in terms of forging load and, above all, final shape of the product. In earlier studies, Deform3D® as well as LS-Dyna® has been applied to model the forging process and in this particular study, Abaqus v6.9 has been used. The "porous" material formulation in Abaqus lets the engineer model cellular materials like metallic foam. However, results could be further improved by fine-tuning the constitutive model of metallic foam. In order to improve upon the results, Deshpande-Fleck model will be implemented by subroutines and compared with the existing Gurson-Tvergaard model.

10. Acknowledgements

The authors would like to thank Theo Verbruggen of Simulia Benelux BV and Renuka Srinivasan of Simulia India Pvt. Ltd. for extending their support for this study.

11. References

1. Deshpande VS, Fleck NA, Isotropic constitutive models for metallic foams, Journal of the Mechanics and Physics of Solids, 2000, 48, 1253–1283.
2. Onck PR, Application of a continuum constitutive model to metallic foam DEN-specimens in compression, International Journal of Mechanical Sciences, 2001, 43, 2947–2959.
3. Gioux G, McCormack TM, Gibson LJ, Failure of aluminum foams under multiaxial loads. International Journal of Mechanical Sciences, 2000, 42, 1097–1117.
4. Hård af Segerstad P, Larsson R and Toll S, A constitutive equation for open-cell cellular solids, including viscoplasticity, damage and deformation induced anisotropy, International Journal of Plasticity, May 2008, 24(5), 896-914.
5. Mulalo Doyoyo and Tomasz Wierzbicki, Experimental studies on the yield behavior of ductile and brittle aluminum foams, International Journal of Plasticity, August 2003, 19(8), 1195-1214.
6. Lorenzo Peroni, Massimiliano Avalle and Marco Peroni, The mechanical behaviour of aluminium foam structures in different loading conditions, International Journal of Impact Engineering, 2008, 35, 644–658.

7. Schmidt I, Deformation induced elasto-plastic anisotropy in metal foams – modelling and simulation , International Journal of Solids and Structures, Volume 41, Issues 24-25, December 2004, Pages 6759-6782.
8. Badiche X, Forest S, Guibert T, Bienvenu Y, Bartout J. -D., Ienny P, Croset M and Bernet H, Mechanical properties and non-homogeneous deformation of open-cell nickel foams: application of the mechanics of cellular solids and of porous materials, Materials Science and Engineering A 30 September 2000, 289(1-2), 276-288.
9. Gibson LJ, Ashby MF, Cellular Solids, Cambridge University Press, Cambridge, 1998.
10. Chen C and Lu TJ, International Journal of Solids and Structures, A phenomenological framework of constitutive modelling for incompressible and compressible elasto-plastic solids, 28 December 2000, 37(52), 7769-7786.
11. Chen C and Fleck NA, Size effects in the constrained deformation of metallic foams, Journal of the Mechanics and Physics of Solids, May 2002, 50(5), 955-977.
12. Jörg Hohe and Wilfried Becker, Geometrically nonlinear stress–strain behavior of hyperelastic solid foams, Computational Materials Science, November 2003, 28(3-4), 443-453.
13. Abaqus v6.9 User Manual, Dassault Systemès, Simulia, 2009.
14. Gurson, AL, Continuum Theory of Ductile Rupture by Void Nucleation and Growth: Part I—Yield Criteria and Flow Rules for Porous Ductile Materials, Journal of Engineering Materials and Technology, 1977, 99, 2–15.
15. Tvergaard V, Influence of Voids on Shear Band Instabilities under Plane Strain Condition, International Journal of Fracture Mechanics, 1981, 17, 389–407.
16. Gagliardi F, Filice L, Umbrello D and Shivpuri R, Forging of metallic foams to reproduce biomechanical components , Materials Science and Engineering A, 2008, 480, 510–516.
17. Gagliardi F, De Napoli L, Filice L and Umbrello D, A comparison among FE models to simulate metallic foams forming – An experimental validation, Materials and Design, 30 (2009), 1282–1287.
18. Filice L, Fratini L, Umbrello D, Mater. Sci. Forum, 2007, 539–543, 1886–1891.
19. Simone AE, Gibson LJ. Aluminum foam produced by liquid-state process. Acta Mater 1998;46:3109–23.
20. Sugimura Y, Meyer J, He MY, Bart-Smith H, Grenstedt J, Evans AG, On the mechanical performance of closed cell AL alloy foams. Acta Mater 1997;45:5245–59.
21. Esen Z and Bor S, Processing of titanium foams using magnesium spacer particles, Scripta Mater. 2007, 56, 341–344.
22. Trendelenburg T, Nishimura H, Claar D, Schaeffler P and Berthold P, Alulight, National Shipbuilding Research Program, presentation by the Panel on Product Development and Materials Technology, Biloxi, MS, 14 February 2008.
23. Raimondi MT and Pietrabissa R, Modelling evaluation of the testing condition influence on the maximum stress induced in a hip prosthesis during ISO 7206 fatigue testing, Med. Eng. Phys., 1999, 21 (5), 353–359.
24. Manisekar K, Narayanasamy R, Malayappan S, Effect of friction on barrelling in square billets of aluminium during cold upset forging, Mater. Des., 2006, 27, 147–155.